Biol. Cybern. 73, 97–111 (1995)

Biological Cybernetics

A model of the neuro-musculo-skeletal system for human locomotion

I. Emergence of basic gait

Gentaro Taga

Department of Pure and Applied Sciences, University of Tokyo, Komaba, Meguro-ku, Tokyo 153, Japan

Received: 29 June 1994/Accepted in revised form: 20 January 1995

Abstract. The generation of human locomotion was examined by linking computational neuroscience with biomechanics from the perspective of nonlinear dynamical theory. We constructed a model of human locomotion, which includes a musculo-skeletal system with 8 segments and 20 muscles, a neural rhythm generator composed of 7 pairs of neural oscillators, and mechanisms for processing and transporting sensory and motor signals. Using a computer simulation, we found that locomotion emerged as a stable limit cycle that was generated by the global entrainment between the musculo-skeletal system, the neural system, and the environment. Moreover, the walking movements of the model could be compared quantitatively with those of experimental studies in humans.

1 Introduction

The study of motor control has previously been dominated by the view that the neural system creates programs for movement which are executed by the musculo-skeletal system. Neuroscience has focused on how the activity of the neural system causes movement of the body. In contrast, biomechanics has focused on the dynamics of the musculo-skeletal system in response to a given set of neural inputs. However, it is difficult to identify which is the cause and which is the effect of movement that is generated through interaction between the neural system, the musculo-skeletal system, and the environment. Therefore, the challenge is to develop a principle which links neural dynamics with effector dynamics.

Studies of human locomotion have focused mainly on musculo-skeletal dynamics. The inverse dynamics method has been used to estimate forces and moment patterns based on a mathematical representation of the body and information on actual human movement (Inman et al. 1981; Winter 1987). On the other hand, the forward dynamics method has been used to simulate movement based on a mathematical representation of the body and a given set of neural inputs (Yamaguchi and Zajac 1990). These studies have clarified the causal relation between neuro muscular activation and motion of the body. However, an understanding of the linkage between neural dynamics and musculo-skeletal dynamics is essential for elucidating the mechanism of the generation and control of locomotion.

Neurophysiological studies of animal locomotion have revealed that the basic rhythm of movement is controlled by rhythm-generating networks in the nervous system, which are called central pattern generators (CPGs) (Delcomyn 1980; Grillner 1985; Selverston 1985). Although isolated CPGs may have the ability to generate rhythmic activities without sensory or descending signals, interaction between CPGs and sensory inputs may be indispensable for locomotion in a natural environment (Bässler 1986; Smith and Zernicke 1987; Cruse 1990). Centrally generated rhythm are entrained by sensory signals which are induced by rhythmic movement of the motor apparatus in animals (Wendler 1974; Grillner and Wallén 1982; Anderson and Grillner 1983; Williams et al. 1990; Grillner and Matsushima 1991; Pearson et al. 1992). This strongly suggests that motor output is an emergent property of dynamic interaction between the neural system, the musculo-skeletal system, and the environment.

As an integrative principle of linkage between neural and musculo-skeletal dynamics, Taga et al. (1991) proposed that 'global entrainment' between the neural and musculo-skeletal systems generates stable and flexible locomotion in an unpredictable environment. A computer simulation demonstrated that the locomotion of a biped with a simple musculo-skeletal system emerged as a limit cycle which was stable against mechanical perturbation and environmental changes. From the point of nonlinear dynamical theory (Haken et al. 1985; Schöner and Kelso 1988), the stability and flexibility of

Part of this paper was presented to IVth International Symposium on Computer Simulation in Biomechanics, Paris, France, July 1, 1993

movement can be attributed to attractor dynamics, which emerges from the dynamic interaction between the various components of the system and the environment. Neural models associated with a body and a mechanical environment have also been examined in other locomotor systems; e.g. fish (Ekeberg 1993), insects (Beer 1990; Kimura et al. 1993), and an artificial leg (Doya and Yoshizawa 1992).

This study is directed towards gaining an understanding of human locomotion. First, we address difficult problems for locomotor control in humans and then propose an integrated model which includes realistic dynamics of the human musculo-skeletal system, neural dynamics of rhythmic pattern generation, and a mechanism of sensorimotor integration to provide dynamic stability for the entire system. We demonstrate that this model produces a stable gait comparable to that seen in humans.

2 Characteristics of human locomotion

From a mechanical point of view, human bodies are inherently unstable, since the center of mass extends beyond the base of support most of the time during walking. Moreover, the movement of the entire body does not always attain dynamic stability even when each joint is perfectly controlled based on a prescribed trajectory, since torques cannot be exerted at the center of pressure (COP) of the ground reaction forces. This condition has been referred to as unpowered degrees of freedom (Vukobratovic and Stokic 1975). Since the motion of unpowered degrees of freedom must be compensated for by the motion of powered degrees of freedom, we need a global strategy to integrate the motion of part of the system and the motion of the entire system simultaneously.

The human body is also characterized by oscillatory dynamics, due to the effects of gravity and inertia. Since locomotion can be defined as a displacement of the body's center of gravity (COG) with respect to the COP, the motion of the entire body can be regarded as the motion of an inverted pendulum. In contrast, the motion of a swinging limb can be regarded as that of a coupled pendulum. It has been shown that the resonant frequency of the system is an important determinant of spontaneous walking (Mochon and McMahon 1980; Holt et al. 1990; McGeer 1993).

When humans are walking in a steady state, the pattern of rotations around all of the joints forms a complex array, with the various joints moving asynchronously with respect to one another (Murray 1967). Each muscle has its own specific pattern of activity during separate phases of the step cycle (Inman et al. 1981). Although the mechanism of reflex in posture and locomotion has been shown to be quite flexible (Stein and Capaday 1988; Dietz 1992), the mechanism by which the central nervous system generates such patterned signals to the muscles and maintains stability are still unclear. On the other hand, the generation of animal locomotion is believed to involve CPGs in the spinal cord which are subdivided into unit generators, each of which principally regulates muscle activity around a single joint (Grillner 1985). In quadruped animals, the hip, knee, and ankel joints are moved in phase, and flexor and extensor muscles are active during the swing and stance phases, respectively, which are markedly different from the complex patterns in humans (Frossberg 1985).

Although autonomous CPGs have not yet been demonstrated in humans, characteristic step-like movements of newborn infants when held upright (McGraw 1940) suggest that innate neural networks for stepping exist in the spinal cord. It is unclear how such networks may develop and generate the mature locomotion of adults (Thelen and Fisher 1982; Forssberg 1985). However, analyses of patterns of EMGs in adult humans during walking also suggest that a few feature signals are sufficient to produce the activity profiles of most of the muscles (Patla 1988). Davis and Vaughan (1993) performed a statistical analysis of 16 EMG signals during walking and showed that the time course of the EMG signals could be accounted for by as few as four patterns: heel-strike, loading response, propulsion, and biphasic factor. Therefore, a CPG for human walking probably exists in some form, although a simple network may not be adequate to generate the specific pattern of the gait.

3 Outline of human locomotion model and control strategy

Figure 1 shows the basic structure of our model of human locomotion. It essentially consists of two dynamical systems: a musculo-skeletal system and a neural rhythm generator composed of neural oscillators. Output signals from the neural rhythm generator induce body movements by activating muscles, while the current state of the musculo-skeletal system and the environment is received by a sensory system and sent to the neural rhythm generator. The processing and transportation of signals in the neural system are assumed to be

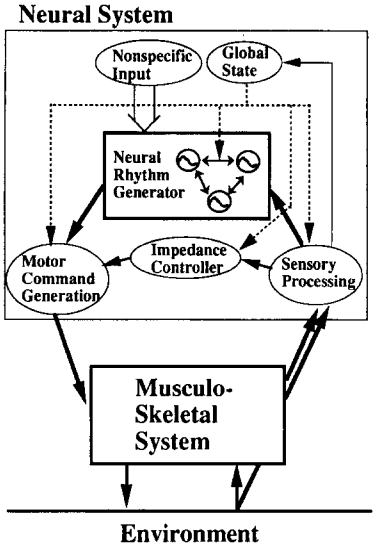

Fig. 1. Model for human locomotion

computational processes. This assumption is valid under the condition that the time required for these processes is short enough to be neglected, as compared with the time required to generate the rhythmic motor commands in the neural rhythm generator.

Since both the neural and musculo-skeletal systems have an oscillatory character, the basic strategy for locomotor control is to establish a stable limit cycle using global entrainment between the two systems (Taga et al. 1991; Taga 1994). Each neural oscillator controls muscles around a single joint and receives sensory signals from the adjacent segments. Although this local interaction between the neural oscillators and body segments contributes to the generation of a limit cycle, entrainment must be established between the neural rhythm generator and a global variable that represents the motion of the entire body and corresponds to the unpowered degrees of freedom. We postulate that the angle of an inverted pendulum used to express the motion of the entire body is computed in the neural system and sent to each of the neural oscillators in such a way that the motion of the entire body can be stabilized through global entrainment.

The mechanical conditions of the limbs change drastically within a gait cycle. This implies that the control process must also change according to the phase of the gait. We assume that a gait can be represented as a sequence of what we call 'global states' and that both the generation of motor commands and sensory processing are modulated by the global states, so that dynamic linking between the neural rhythm generator and the musculo-skeletal system is established and maintained. The global states also control the coupling among the neural oscillators, which enables generation of a complex pattern of activity with appropriate timing. The higher center of the neural system regulates the activity level of the neural rhythm generator by sending a nonspecific input. In parallel with the control of rhythmic movements, we assume a controller of mechanical impedance (e.g., stiffness and viscosity), which maintains the upper body in an upright posture and prevents limbs in the stance phase from collapsing.

4 Model of human locomotion

4.1 Body dynamics and muscle action

Various models of bipedal locomotion have been studied (Vukobratovic and Stokic 1975; Onyshko and Winter 1980; Flashner et al. 1987; Pandy and Berme 1988; Yamaguchi and Zajac 1990; Taga et al. 1991). To reproduce human locomotion not only qualitatively but also quantitatively, the body in the present model is represented by eight segments, with two complete three-segment lower limbs and two segments in the upper body, as shown in Fig. 2. Each foot is represented by a triangle of appropriate proportions. The interaction between the foot and the ground is modeled as a spring and damper acting at the heels and toes. The rest positions of the elastic forces are reset each time the heels and/or the toes touch the ground (Raibert 1984). Torques

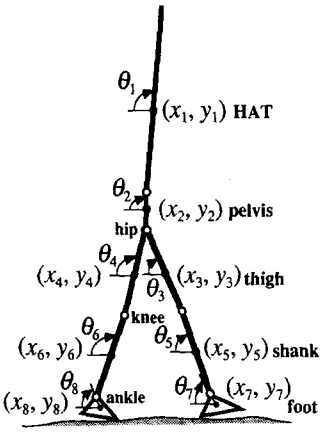

Fig. 2. The model of the human body, composed of the *HAT* (head, arms, and trunk), pelvis, thigh, shank, and foot. There are seven joints, two each at the hips, knees, and ankles, and one at the trunk

exerted by passive joint structures acting across the joints are assumed to limit the ranges of joint flexion and extension (Davy and Audu 1987). The passive torques are small within certain ranges of the joint angles, while large passive torques are exerted if the joint angles exceed the limit. Parameters of the body segments are arbitrarily assigned based on an adult man. The model is confined to movement in the sagittal plane.

The equation of motion are derived by means of the Newton-Euler method. Their general form can be written as

$$\begin{aligned} M\ddot{\mathbf{x}} &= A_x\mathbf{F}_x + A_{gx}\mathbf{F}_{gx} \\ M\ddot{\mathbf{y}} &= A_y\mathbf{F}_y + A_{gy}\mathbf{F}_{gy} - \mathbf{G}, \\ I\ddot{\theta} &= B(\theta)\mathbf{F} + B_g(\theta)\mathbf{F}_g + C_p\mathbf{T}_p(\theta, \dot{\theta}) + C_a\mathbf{T}_a \end{aligned} \tag{1}$$

where $\mathbf{x}, \mathbf{y}$ and θ are (8×1) vectors of the horizontal positions, vertical positions, and inertial angles of the eight segments; $\mathbf{F}_x$ and $\mathbf{F}_y$ are (7×1) vectors of constraint forces in the horizontal and vertical direction; $\mathbf{F}_{gx}$ and $\mathbf{F}_{gy}$ are (4×1) vectors of ground reaction forces on the feet in the horizontal and vertical directions; $\mathbf{T}_p$ and $\mathbf{T}_a$ are (7×1) vectors of passive torques exerted by passive joint structures and active torques exerted by muscles; M and I are (8×8) diagonal matrices of mass and moment of inertia; A_x and A_y are (8×7) matrices with constant values; A_{gx} and A_{gy} are (8×4) matrices with constant values; $\mathbf{G}$ is a (8×1) vector of gravitational forces on each segment; $\mathbf{F} = (\mathbf{F}_x^t, \mathbf{F}_y^t)^t$, $\mathbf{F}_g = (\mathbf{F}_{gx}^t, \mathbf{F}_{gy}^t)^t$; $B(\theta)$ is a (8×14) matrix; $B_g(\theta)$ is a (8×8) matrix; and C_p and C_a are (8×7) matrices.

Constraint forces acting at the joints can be eliminated by using equations of kinematic constraints. The general form of the kinematic constraints can be written as

$$\begin{aligned} D_x\mathbf{x} &= \mathbf{E}_x(\theta) \\ D_y\mathbf{y} &= \mathbf{E}_y(\theta) \end{aligned} \tag{2}$$

where D_x and D_y are (7×8) matrices; and $\mathbf{E}_x$ and $\mathbf{E}_y$ are (8×1) vectors which are functions of θ. The method of elimination of the constraint forces is given in the Appendix.

The active torques at the joints are generated by 20 muscles. Although an active torque exerted by a muscle should be given by the muscle force multiplied by its moment arm, which changes according to the displacement of the joint angle (Hatze 1976), it is assumed, for simplicity, that the moment arms of the muscles have constant values and that muscle forces are proportional to the output of the neural system. Therefore, each muscle produces a muscle torque at a specific joint in proportion to the output of the neural system. Since the double-joint muscles have different values for the moment arms of the different joints, their muscle torques are assumed to be generated in certain proportions. The active torques at each joint can be represented by the function of the muscle torques as

$$T_{ai} = \sum_{j=1}^{20} C_{ij} T_{mj}, \quad (i = 1, 7) \tag{3}$$

where C_{ij} is a (7×20) matrix and T_{mj} is a muscle torque of the jth muscle.

4.2 Rhythm generation and sensory processing

The basic rhythm for locomotion is assumed to be generated by neural oscillators that consist of two tonically excited 'neurons' with a self-inhibition effect, which are linked reciprocally via inhibitory connections (Matsuoka 1985). This structure is similar to several models for spinal stepping generators (Miller and Scott 1977; Kawahara and Mori 1982) in that one neuron drives the flexor while the other drives the extensor. A neural oscillator is represented by differential equation as

$$\begin{aligned} \tau_i \dot{u}_i &= -u_i - \beta f(v_i) + \sum_{j \neq i} w_{ij} f(u_j) + u_0, \\ \dot{\tau}_i \dot{v}_i &= -v_i + f(u_i), \\ (f(u) &= \max(0, u)), \quad (i = 1, 2) \end{aligned} \tag{4}$$

where u_i is the inner state of the ith neuron; v_i is a variable which represents the degree of the adaptation or self-inhibition effect of the ith neuron; τ_i and τ'_i are time constants of the inner state and the adaptation effect of the ith neuron, respectively; β is a coefficient of the adaptation effect; w_{ij} is a connecting weight from the jth neuron to the ith neuron; and u_0 is an external input with a constant rate. The appearance of a stable limit cycle can be derived analytically (Matsuoka 1985). By using this neural oscillator, we constructed a model neural system which reproduces human locomotion.

It is still unclear how the human neural system represents and integrates different types of sensory information, such as somatosensory information including muscle proprioception, joint, and cutaneous afferents, vestibular information, and visual information, during locomotor control. In this model, rather than describing the neural events involved in this sensory processing, we assume that the representation and transformation of the sensory information involve a simple computational process. We postulate that the angles and angular velocities of the body segments in an earth-fixed frame of reference, ground reaction forces, and positions of the foot in contact with the ground are available for this processing. If the orientation of gravity can be sensed by the vestibular or visual system, the inertial angles of the segments can be easily obtained from the proprioceptive information on the joint angles.

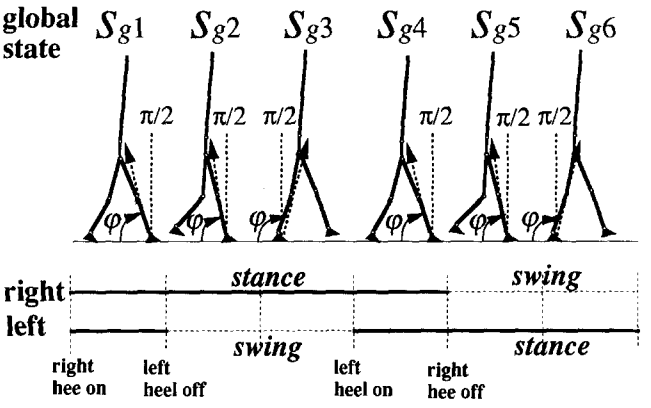

Fig. 3. Global pattern of movement within a gait cycle represented by a cyclic sequence of the global states. A gait cycle is defined as the time interval between successive instances of initial foot-to-floor contact with the same foot. s_{gk} is determined by the global angle φ and the position of the foot contacting the ground. The single-support phase is divided into two periods: the first half, when the global angle is less than $\pi/2$, and the second half, when the global angle exceeds $\pi/2$

Sensing limb movement in the context of motion of the entire body is essential to locomotor control because of the existence of unpowered degrees of freedom (Vukobratovic and Stokic 1975). Since human walking is characterized by displacement of the body's COG with respect to the COP of the ground reaction forces, the orientation of the vector from the COP to the COG in an earth-fixed coordinate represents global information and is referred to here as the 'global angle'. It can be defined as

$$\phi = \cos^{-1}[(x_{cp} - x_{cg})/\{(x_{cp} - x_{cg})^2 + (y_{cg} - y_{cp})^2\}^{\frac{1}{2}}] \tag{5}$$

where (x_{cg}, y_{cg}) and (x_{cp}, y_{cp}) are the coordinates of the COG and COP, respectively. The global angle can be obtained using proprioceptive and somatic information.

4.3 Generation of gait pattern

The global features of the human gait can be characterized by the displacement of the global angle and the alternation of the foot contacting the ground. In the neural system, the gait pattern is assumed to be represented as a cyclic sequence of six states, as shown in Fig. 3. These discrete states are further assumed to prescribe control actions to be taken during the state. We define 'global state' by $s_{gk} (k = 1, 6)$, which can be chosen such that $s_{gk} = 1$ only when the current state is the kth state of the gait cycle; otherwise, $s_{gk} = 0$. The gait pattern is then

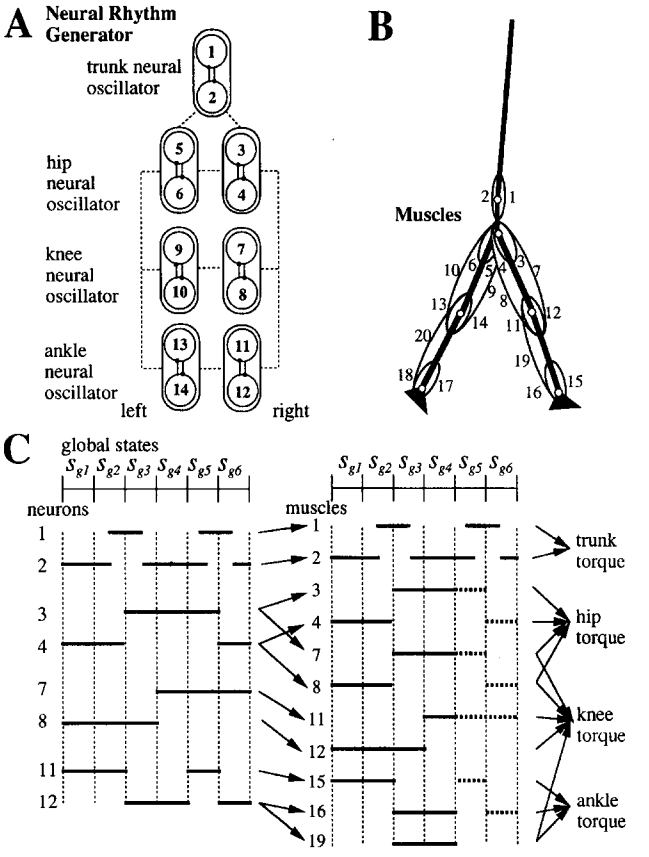

Fig. 4. **A** Neural rhythm generator composed of seven neural oscillators. The hip, knee, and ankle oscillators primarily induce action of single-joint muscles of the corresponding joints, while the hip oscillator activates the hip-knee double-joint muscle, and the ankle oscillator activates the knee-ankle double-joint muscle. **B** Schematic representation of the model of the muscle groups. There are six single-joint muscles and three double-joint muscles for each of the limbs and two for the upper body. *1*, Rectus abdominis; *2*, erector spinae; *3*, *5*, iliopsoas; *4*, *6*, gluteus maximus; *7*, *9*, rectus femoris; *8*, *10*, hamstrings; *11*, *13*, biceps femoris; *12*, *14*, vastus; *15*, *17*, tibialis anterior; *16*, *18*, soleus; *19*, *20*, gastrocnemius. **C** Hypothetical diagram of active periods of neurons and muscles. Since normal walking is symmetrical, the pattern is shown only for the right limb. *Thick lines* show the periods during which the neurons and muscles are activated. *Dashed lines* in the muscle activation pattern show periods of relatively weak activation

specified not by the precise trajectories of each segment, but by the global feature of the movement.

The neural rhythm generator consists of seven neural oscillators, with one neural oscillator for the trunk and a pair of three neural oscillators for the limbs (Fig. 4A), each of which induces the action of specific muscles (Fig. 4B). The two neurons in the neural oscillators alternately activate the antagonist muscles. The values of the parameters of the neural oscillators are roughly estimated such that their rhythmic activity becomes resonant with the oscillation of the limbs.

Figure 4C illustrates a hypothetical diagram of active periods of the neurons and muscles within a gait cycle during steady walking. The trunk oscillator excites itself twice during each gait cycle with a specific relationship to the oscillation of the hip oscillators on both sides. The hip and knee oscillators have a phase difference of 1/6 period, which causes an appropriate pattern of muscle activation at these joints. The timing of the activation of the hip extensors is associated with the foot's contact with the ground, while the knee extensors are active and carry the load of the body during the first half of the support phase. The extensor neuron of the ankle oscillator is active during the second half of the single-support phase and the succeeding double-support phase, which is important in producing a forward thrust of the body by the strong activation of the extensor muscle of the ankle.

Inhibitory connections are incorporated between the left and right neural oscillators at each joint, since activation of the neural oscillators on the left and right sides should be phase-locked in an antiphase relationship. However, it is difficult to realize complex phase relationships among the neural oscillators on the ipsilateral side by using only fixed connections. Therefore, we assume that the couplings between the ipsilateral oscillators are not continuous, but rather are active only within selected states in the gait cycle. Each global state represented by s_{gk} determines a set of connections among the neurons. The input signal to the ith neuron from the other neurons is given in a general form as

$$Q_i = \sum_{k=1}^{6} s_{gk} \sum_{j=1}^{14} w_{ij}^{k} f(u_j) \tag{6}$$

where w_{ij}^{k} is the strength of the connection from the jth neuron to the ith neuron at the kth state in the gait cycle. The couplings are chosen such that the neurons which should be active in a global state are mutually excited during the global state, while the neurons that should not be active are inhibited by the other active neurons. Such phase-dependent coupling among oscillators has been suggested in some locomotor systems of animals (Cruse 1990).

4.4 Sensorimotor integration

How sensory information interacts with the central mechanism is extremely important in locomotor control. Motion-dependent information about the body is assumed to be modulated and sent to the neural rhythm generator. The angles of the body segments in an earth-fixed frame of reference are sent to the neurons of the adjacent neural oscillators in such a way that the displacement of the angles on one side with reference to the vertical direction suppresses the neurons which induce torque in the same direction and enhances the neurons which induce torque in the opposite direction. Moreover, these signals are modulated by information about the 'global states' so that angular information is sent to the neural rhythm generator within selected periods of the global states. Thus, the mechanism postulated in this model is consistent with that in the functional stretch reflex (Matthews 1991). Phase-dependent modulations of afferent signals have been demonstrated in humans (Stein and Capady 1988) and in cats (Forssberg 1979).

To establish global stability, we assume that the current states of the global angle and angular velocities are sent to the neural rhythm generator so that the rhythmic

activity of the neural rhythm generator and the movement of the inverted pendulum represented by the global angle are mutually entrained. Studies on EMGs during walking suggest that the global information may be used in some form to coordinate multiple muscles. For example, unilateral perturbations to limbs are followed by a bilateral response of EMG activity with similar latencies on both sides (Berger et al. 1984).

The local and global sensory information that is sent to the ith neuron can be written in a general form as

$$S_i = \sum_{k=1}^{6} s_{gk} \Bigg[\sum_{j=1}^{8} \{q_{aij}^k(\theta_j - \theta_{0j}) + q_{bij}^k \dot{\theta}_j\} + q_{ci}^k(\phi - \pi/2) + q_{di}^k f(\pi/2 - \phi) + q_{ei}^k \dot{\phi} \Bigg] \quad (7)$$

where q_{aij}^k, q_{bij}^k, q_{ci}^k, q_{di}^k and q_{ei}^k are constant parameters.

4.5 Generation of motor commands in the neural system

The dynamics of the neural rhythm generator, including the state-dependent interaction among the neural oscillators and the sensory input, can be represented by the following differential equations:

$$\tau_i \dot{u}_i = -u_i - \beta f(v_i) + \sum_{j=1}^{14} w_{ij}^0 f(u_j) + u_0 + Q_i + S_i,$$
$$\dot{\tau}_i \dot{v}_i = -v_i + f(u_i) \quad (8)$$
$$(f(u) = \max(0, u)), \quad (i = 1, 14)$$

The output of the neural rhythm generator is finally transformed into the motor command that induces muscle activity. Since the output signals of the neural rhythm generator do not contain detailed information about the magnitude of specific muscle activity, we assume that the output signals multiplied by specific coefficients produce the specific muscle torques. The coefficients are also assumed to be temporally modulated by information about the global state. In general, the coefficients are small in the swing phase and large in the stance phase, which allows appropriate torques to be generated. We call this part a rhythmic force controller.

Together with the rhythmic control of the body by the neural rhythm generator, the control of mechanical impedance (Hogan 1985) is needed to generate enough torques of the joints to maintain posture during walking. We postulate that the stiffness and viscosity of the joints can be controlled by the impedance controller which generates motor commands to the muscles proportional to deviation of the segment angles from preset angles and to angular velocities during appropriate periods of the gait cycle. At the trunk and hip joints, visco-elastic torques are always produced to maintain the upright posture of the upper body. At the knee joints, the stiffness and viscosity are increased during the stance phase to avoid collapse. At the ankle joints, only viscous torques are produced during the stance phase to prevent the development of an excess momentum of the whole body around the ankle joint. In case there is no output from the neural rhythm generator and both limbs touch the ground, the model could maintain a standing posture by increasing the stiffness and viscosity at all of the joints. In general, the stiffness and viscosity of joints can be increased by the co-activation of antagonistic muscles. Neurophysiological studies on quadruped animals suggest the presence of parallel pathways of control of rhythmic movements and postures (Mori 1987).

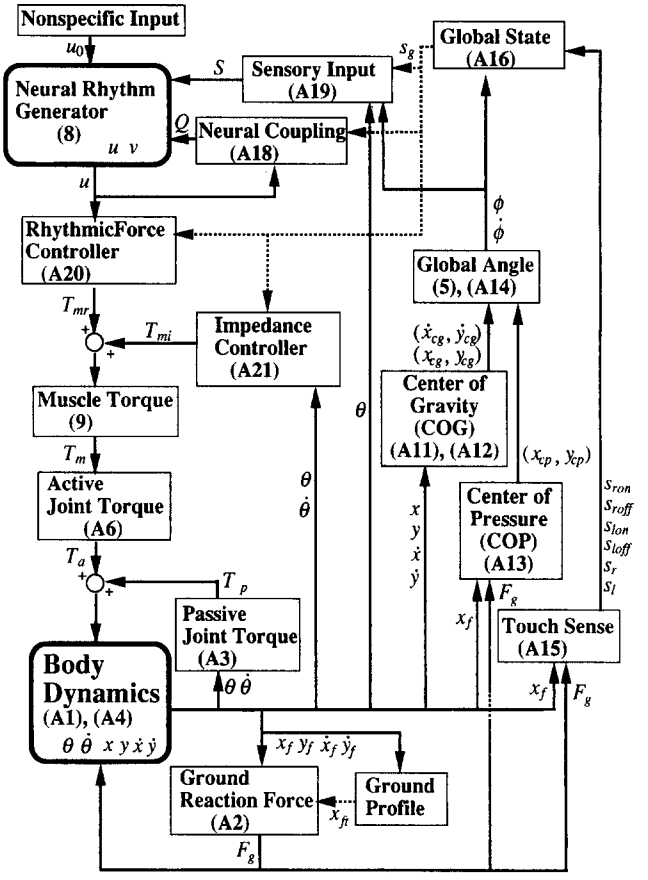

Fig. 5. Block diagram of the neuro-musculo-skeletal system for human locomotion

Both of the motor commands are summed and sent to the muscles to generate joint torques. The muscle torques are represented as

$$T_{mi} = T_{mri}(\mathbf{u}, \mathbf{s}_g) + T_{mi\,i}(\theta, \dot{\theta}, \mathbf{s}_g), \quad (i = 1, 20) \quad (9)$$

where T_{mi} is the torque generated by the ith muscle, T_{mri} is the ith muscle's torque originating from the neural rhythm generator, and $T_{mi\,i}$ is the ith muscle's torque due to the impedance controller.

4.6 Numerical methods

A block diagram of the entire system is illustrated in Fig. 5. Since the entire system is composed of two dynamical systems, we need essentially to solve (1) and (8) in parallel. Equation (1), which describes the segment dynamics, cannot be integrated in a straightforward manner because the constraint forces among the segments are unknown. By reducing these forces using (2), we obtain

differential equations (18) in the Appendix, which can be integrated if the active torques are given. Equation (8), which describes the neural dynamics, can be integrated if we know the state variables of (18). Therefore, we can numerically integrate (18) and (8) in parallel. We used the fourth-order Runge-Kutta-Gill method for this integration. The time step for the integration was 0.25 ms. The inverse matrix in (18) was solved using the Gauss-Jordan method at every time step for the integration. To avoid numerical errors, we used speed stabilization through projection (Ekeberg 1993), since this system has a stiff character, which causes violations of the kinematic constraints. Calculations were performed on the HITAC S3800 at the Computer Center of the University of Tokyo.

Obtaining a stable gait required a balance of parameter values: (a) the body parameters, (b) the parameters in the neural oscillators, (c) the strength of the neural connections, (d) the magnitude of the coefficients in the rhythmic force controller, (e) the strength of the sensory inputs, and (f) the impedance parameters. The values of (a) were determined based on data from an adult man. The values of (b) were chosen such that the neural oscillator has a stable limit cycle, a condition which can be derived analytically. Since a cycle period of the neural oscillator is proportional to the time constants of the neurons, they were adjusted to the values of a resonance frequency of a simple pendulum equivalent of the lower limb. The values of (c) were arbitrarily chosen so that the neural oscillators were entrained with each other. We can roughly estimate the values of (d) based on the proportion between the amplitude of the neural oscillators and the experimentally measured values of the muscle torques. We can also estimate the range of values of (e), since global entrainment never occurred between the neural and mechanical system when they were too weak, while the stability of the limit cycle was broken when they were too strong. The values of (f) were chosen such that the impedance controller produced enough torques to maintain posture. After estimating all of these parameters roughly, we fixed the values of (a), (b), (c), and (f) and then conducted fine tuning of the values of (d) and (e) through a trial-and-error process. At the initial point of simulation, the body was assumed to have a forward velocity with a natural configuration of the segments, and the initial conditions of the neurons were arbitrarily chosen. We fixed the initial conditions during parameter tuning.

5 Generation of human gait

Given a set of parameters and the initial conditions shown in the Appendix, the solutions of the differential equations converged to a steady state. A stick figure of the walking movement (Fig. 6A) demonstrates that steady walking was realized and maintained. The pattern of walking within a gait cycle in Fig. 6B shows features that are characteristic of the human gait. A gait cycle begins with the heel striking the ground. Once the entire foot makes contact with the ground, the limb bears the weight of the entire body, while the other limb swings and clears the ground. The body is then thrust forward by

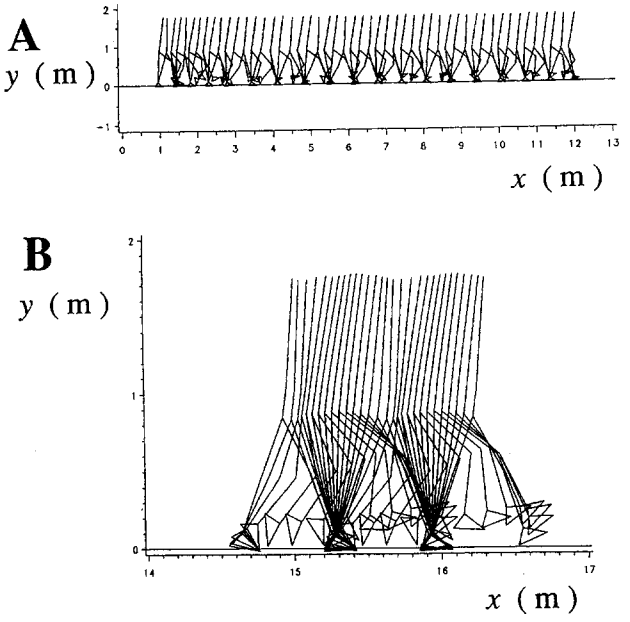

Fig. 6. **A** Stick figure of walking movement. Given a set of initial conditions, the walking movement converged to a steady state. The stick figure was traced every 0.2 s. **B** Stick figure of walking movement in the steady state within a gait cycle. The stick figure was traced every 0.01 s

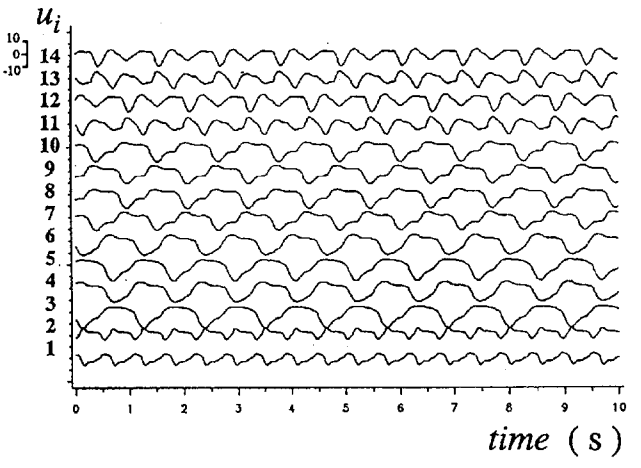

Fig. 7. Activities of the neural oscillators. The time courses of the state variables of each neuron are shown

a push-off movement in the ankle joint. The activity of the neural rhythm generator shown in Fig. 7 demonstrates that the activity of each neuron also converged to a steady state. Such behavior is characteristic of a stable limit cycle with an attractive orbit.

Phase plane plots of the motion of the inertial angles of the body segments and the activity of the neural oscillators display topological forms of motion, as shown in Fig. 8. The transient behavior of the phase plane trajectories that are attracted to a stable limit cycle is shown in Fig. 8A. After several gait cycles, the trajectories were completely attracted to the closed orbit shown in Fig. 8B. From these phase plane plots, it is clear that the limit cycle is generated in a state space that consists of the musculoskeletal system and the neural system. The convergence to the steady state occurred more rapidly in the

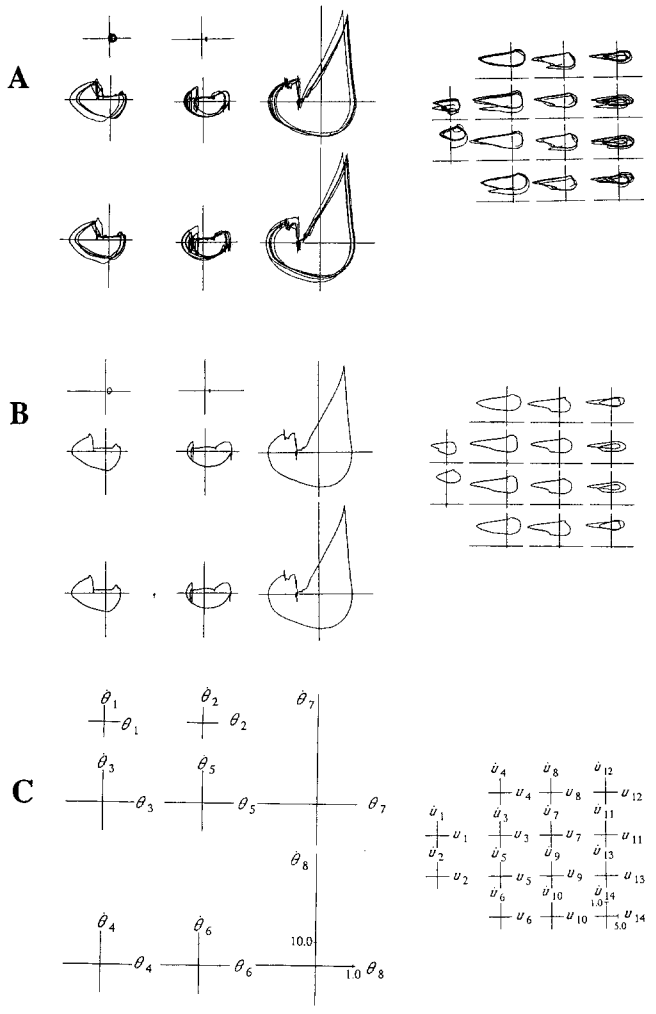

Fig. 8A–C. Phase portraits. For the motion of a segment of the musculo-skeletal system, the phase portrait represents the segment's angle and its velocity. For the activity of a neural oscillator of the neural system, it represents the state variable and its first derivative. **A** Transient state to a steady state. Given the initial condition, trajectories for the first 10 s are shown. **B** Phase portraits in the steady state. Trajectories for the second 10 s are shown. **C** Definition of coordinates of the phase plane plots presented in **A** and **B**

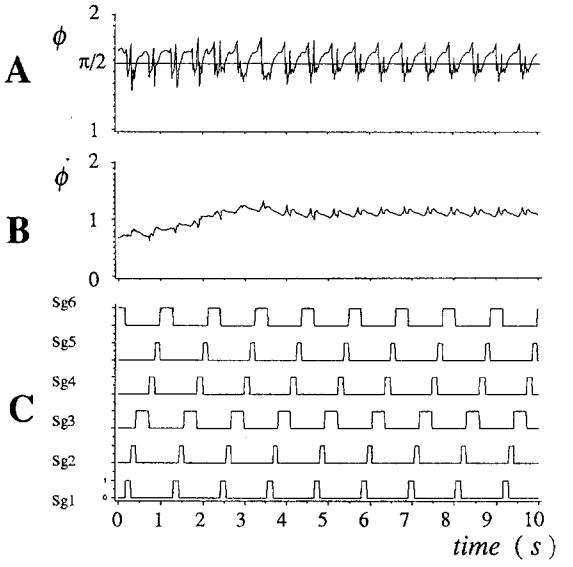

Fig. 9. A Displacement of the global angle; **B** displacement of global angular velocity; **C** displacement of the global state

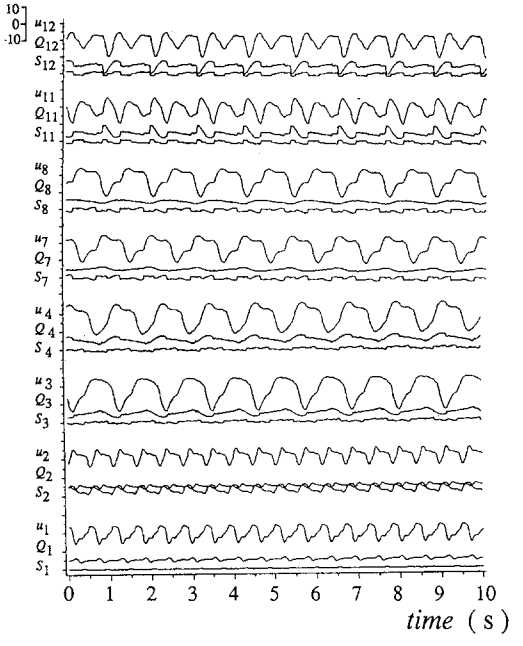

Fig. 10. Synchronization among the activity of a neural oscillator, input signals from other neural oscillators, and sensory signals. u_i is the activity of the ith neuron, Q_i is the sum of the input signals from other neural oscillators to the ith neuron, and S_i is the sum of the sensory input signals of the ith neuron

thigh and shank segments than in the foot segment. Correspondingly, the hip and knee oscillators converged more quickly than the foot oscillators.

Figure 9A and B shows the time course of the global angle and the global angular velocity. The behavior is characterized by a strong convergence to a steady state, which indicates that global stability was established throughout the entire system. The time course of the global states in Fig. 9C shows that the walking movement was realized as the cyclic sequence of global states prescribed in Fig. 3. The temporal relationship between the activity of a neuron and its inputs is demonstrated in Fig. 10, in which the input signals from the other neurons and those from the sensory system are shown separately. For each of the neurons, the profile of the activity almost coincides with that of the input signals. This clearly indicates that global entrainment occurs between the activity of the neural rhythm generator and the sensory signals. Contrary to the conventional assumption that the system regulates limb movement, dynamic interaction among the neural system, the musculo-skeletal system, and the environment generates locomotion as an emergent property.

To test the robustness of the model, we examined whether the limit cycle was maintained or not when a certain set of parameters was uniformly changed by simultaneously increasing or decreasing their values. By conducting systematic trials, it was found that the limit

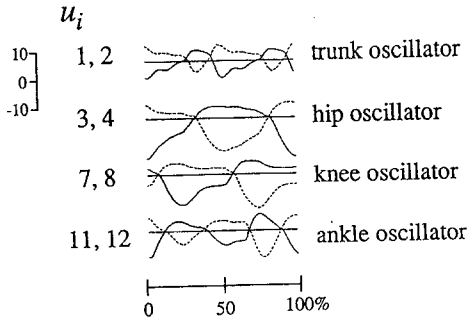

Fig. 11. Profile of the activities of neurons within a gait cycle. Time is normalized by the time for a gait cycle: 0% and 100% indicate when the right heel strikes the ground

cycle remained stable for changes in the strength of the neural connections (− 50% to + 100%), sensory inputs (− 15% to + 35%), and impedance parameters (− 20% to + 50%). In contrast, the range of parameters was relatively narrow for the coefficients of the rhythmic force controller (± 10%) and the time constants of the neurons (± 10%). Since the limit cycle had an orbital stability, it was robust against a small change in the initial conditions. The effect of perturbations to the body during walking will be extensively examined in the companion paper. How a steady gait is generated starting from a quiet-standing posture should be the subject of a future study.

6 Characteristics of various variables in the steady gait

We will now consider time courses of various variables within a gait cycle when the motion of the system has reached a steady state. Since the walking movement is symmetrical under normal conditions, only the variables on one side are shown. Some of these variables can be directly compared to values that have been measured and/or predicted by experiments.

Patterns of the activities of the trunk oscillator and the limb oscillators for the right limb are shown in Fig. 11. A phase relationship among the neural oscillators, which was prescribed in Fig. 4, was obtained in the simulation. This suggest that a similar pattern of neural activity may be generated in the human nervous system.

Figure 12 shows profiles of the muscle torques produced by the neural rhythm generator, those produced by the impedance controller, and the total muscle torques. The output of the neural rhythm generator essentially produced rhythmic action of the muscles in appropriate periods of the gait cycle, i.e., bearing the weight of the body by the hip and knee extensors in the early stance phase, propulsion of the body by the ankle extensors in the late stance phase, controlling the clearance of the foot by the ankle flexors during the swing phase, and controlling the step length by the hip and knee double-joint muscles of the swinging limb. The impedance controller produces a large amount of torque in the trunk and hip muscles to maintain the upright posture of the upper part of the body. In the ankle muscles, the impedance controller produces torque to resist rapid plantar flexion of the

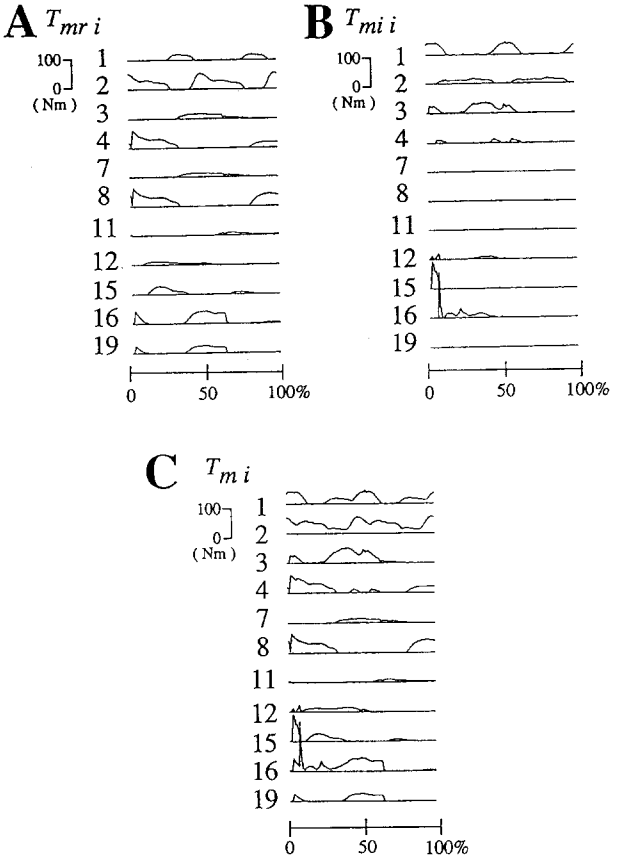

Fig. 12. Profile of the muscle torques within a gait cycle: **A** muscle torques generated by the neural rhythm generator through the rhythmic force controller; **B** muscle torques generated by the impedance controller; **C** total muscle torques

ankle after heel strike. The profile of the muscle torques can be qualitatively compared with predicted patterns of muscle forces (Crowninshield and Brand 1981; Davy and Audu 1987; Yamazaki 1991). It is also possible to compare the muscle torques with measured EMG patterns (Inman et al. 1981; Nilsson et al. 1985), although it is difficult to demonstrate definite relationships between them because of the complex dynamics of the muscles.

Figure 13 shows the active torques exerted by the muscles, the passive torques exerted by the passive joint structure, and the total joint torques. In the knee joint, a considerable amount of the passive torque which restricted hyperextension made a significant contribution to the total joint torque (Yoon and Mansour 1982). In the other joints, the contribution of the passive torque to the total was small. The total joint torques can be compared with those estimated by the inverse dynamics method (Inman et al. 1981). The joint torques acting during the swing phase are small compared with those during the stance phase. The large extensor torque at the ankle in the late stance phase in this model shows good agreement with experimental values.

The displacement of the angles in each segment is shown in Fig. 14A. There was good agreement between the simulated values and those observed in human subjects (Inman et al. 1981). In particular, this model

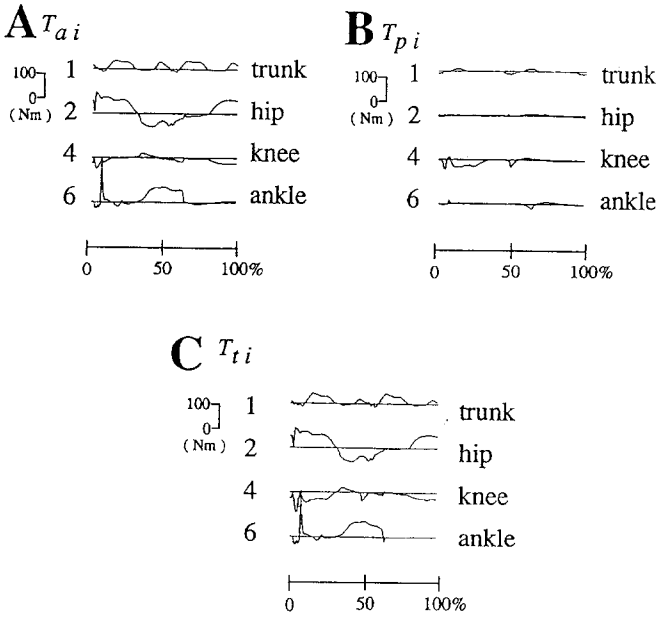

Fig. 13A–C. Profiles of the joint torques within a gait cycle. The positive values show extensor torques. **A** Active joint torques generated by the muscles. **B** Passive joint torques generated by the passive structure of the joints. **C** Total joint torques

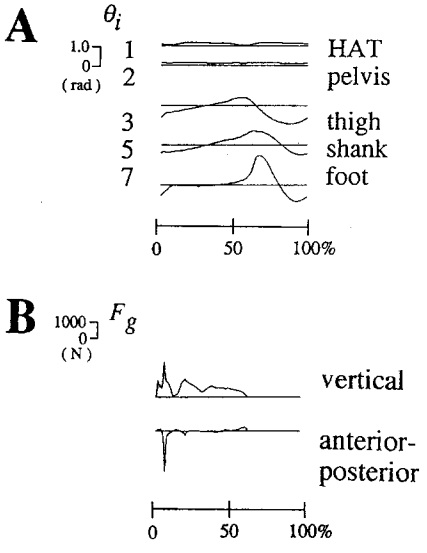

Fig. 14. **A** Profiles of the displacement of the body segments within a gait cycle. **B** Profiles of the ground reaction forces within a gait cycle

reproduced the complex coordination between the shank and the foot in humans.

Figure 14B shows the profiles of the ground reaction forces in the vertical and anterior-posterior directions, which can be compared with those of experimental values measured by force plates (Nilsson and Thorstensson 1989). The force in the anterior-posterior direction acted to decelerate the body and to facilitate weight transfer over the single support limb in the first half of the stance phase, while it acted to accelerate the body for forward progression in the second half of the stance phase. The force in the vertical direction had triple peaks: the first impulsive components of the forces were caused by the collision-type contact between the foot and the ground, which were not typically observed in human experiments, while the second and the third peaks correspond to the dual peaks of experimental values.

7 Discussion

We have shown that the walking movement of our model emerges from dynamic interaction through global entrainment among the neural and musculo-skeletal systems and the environment. The output of the model fully reproduced the complex phenomena of human locomotion. Most of the simulated variables were comparable to the experimental variables in human subjects, although precise matching should be a subject of future study. The process by which human locomotion is controlled can be partly validated by phase plane plots of experimental data of the motion of body segments during walking, which display the characteristics of a limit cycle attractor (Clark and Phillips 1993). It is still an open question of how to validate the neural part of the model in the strict sense.

Since we cannot determine the actual structure and parameters of the neural system at present, this model should be considered a computational theory rather than a direct model of the actual neural system. However, this neural model using neural rhythm generators can provide a framework for understanding the functional role of the neural system in locomotor control. The ability of newborn infants to make stepping movements suggests that a rhythm-generating network is present within the spinal cord in some form, as has been demonstrated in animals, although gait patterns of subjects with cerebral palsy are strikingly different from those of normal subjects (Leonard et al. 1991). These facts indicate that the motor cortex is involved in the generation of normal gait patterns. Therefore, the neural rhythm generator in this model is not necessarily confined to the spinal cord. The cerebellum is also essential for locomotor control by virtue of the sensory information it receives and the influence it has on motor commands (Arshavsky et al. 1984). The cerebral cortex and the cerebellum, as well as the spinal cord, may be involved in the representation of the global angle, state-dependent coupling among the neural oscillators, state-dependent sensorimotor processing, and all of the other assumptions in this model.

The assumption that the angles of each segment in an earth-fixed frame of reference are available to the system plays an essential role in stability during locomotion, although these angles must be transformed from proprioceptive information about the joint angles, as well as from vestibular and visual information. This computation is not as complicated as the transformation of the positions of body segments in earth-fixed coordinates to the joint angles in body-fixed coordinates, which

typically arises in cases of visually guided reaching movements (Soechting and Flanders 1992). Another important assumption in this model is the representation of the global angle. Studies of posture control in humans and animals have suggested that the central nervous system may use global variables such as body configurations (Nashner and McCollum 1985; Maioli and Poppele 1991) and directions of ground reaction forces (Macpherson 1988). Our results indicate that the global variable of the body in an earth-fixed reference frame may be represented in the central nervous system and that it can be stabilized through global entrainment.

Although the dynamics of the muscles were neglected in this model, they should play an important role in locomotor control. In running, humans particularly use elastic properties of muscle tendons and ligaments to produce the vertical movements needed in jumping and to store kinetic energy when their feet strike the ground (McMahon 1984). Along these lines, Raibert (1984) constructed a hopping machine with one leg, in which the dynamic interaction between the elastic properties of the leg and the controller generated stable hopping. In this model of walking, the interaction between the inertial properties of the limbs and the neural system produced stable walking. Therefore, locomotion emerged from the real-time interaction between the neural and mechanical dynamics without a priori limitations on prescribed trajectories of movements, which is in marked contrast to the conventional control theory.

This model may be extended to explore a variety of phenomena related to the control of locomotion. Disorder of gait, which might be caused by neurological disease or musculo-skeletal impairment, can be approached from the perspective of nonlinear dynamics. Phase plane plots of limb segments obtained from subjects with neurological disease show variable trajectories and a reduced tendency to converge to an attractor (Winstein and Garfinkel 1989). In a previous paper, it was shown that a model of a simple biped with considerable time delays in transporting and processing information between the neural system and the musculo-skeletal system generated a chaotic attractor of gait (Taga 1994). Such attractor dynamics may also provide insight into the developmental aspects of locomotion, since the development of infant locomotion can be characterized as a process of seeking stable solutions of walking, which would be given as a result of cooperative interaction between the neural and musculo-skeletal systems and the environment (Thelen 1988; Clark and Phillips 1993).

In the accompanied paper, we will further demonstrate the extreme adaptability of locomotion of this model under various constraints of the environment and tasks.

Acknowledgements. This research was supported by fellowships of the Japan Society for the Promotion of Science for Japanese Junior Scientists and by Grant-in-Aid for Scientific Research (No. 2729) from the Ministry of Education, Science and Culture, Japan. I would like to thank Profs. H. Shimizu and Y. Yamaguchi for their valuable discussions, T. Wadden for his suggestions regarding numerical methods, and Dr. J. J. Collins for his comments on this manuscript.

Appendix

A The equations of motion for the body segments

The equations of motion for the body segments are derived by means of the Newton-Euler method.

$$
\begin{aligned}
&m_H\ddot{x}_1 = F_{x1},\\
&m_H\ddot{y}_1 = F_{y1} - m_H g,\\
&I_H\ddot{\theta}_1 = -F_{x1}l_{H2}\sin\theta_1 - F_{y1}l_{H2}\cos\theta_1 - T_{p1} - T_{a1},\\
&m_p\ddot{x}_2 = -F_{x1} + F_{x2} + F_{x3},\\
&m_p\ddot{y}_2 = -F_{y1} + F_{y2} + F_{y3} - m_p g,\\
&I_p\ddot{\theta}_2 = -F_{x1}l_p\sin\theta_2 - F_{y1}l_p\cos\theta_2 - F_{x2}l_p\sin\theta_2\\
&\qquad - F_{y2}l_p\cos\theta_2 - F_{x3}l_p\sin\theta_2 - F_{y3}l_p\cos\theta_2\\
&\qquad + T_{p1} - T_{p2} - T_{p3} + T_{a1} - T_{a2} - T_{a3},\\
&m_t\ddot{x}_3 = -F_{x2} + F_{x4},\\
&m_t\ddot{y}_3 = -F_{y2} + F_{y4} - m_t g,\\
&I_t\ddot{\theta}_3 = -F_{x2}l_t\sin\theta_3 - F_{y2}l_t\cos\theta_3 - F_{x4}l_t\sin\theta_3 - F_{y4}l_t\cos\theta_3\\
&\qquad + T_{p2} + T_{p4} + T_{a2} + T_{a4},\\
&m_t\ddot{x}_4 = -F_{x3} + F_{x5},\\
&m_t\ddot{y}_4 = -F_{y3} + F_{y5} - m_t g,\\
&I_t\ddot{\theta}_4 = -F_{x3}l_t\sin\theta_4 - F_{y3}l_t\cos\theta_4 - F_{x5}l_t\sin\theta_4 - F_{y5}l_t\cos\theta_4\\
&\qquad + T_{p3} + T_{p5} + T_{a3} + T_{a5},\\
&m_s\ddot{x}_5 = -F_{x4} + F_{x6},\\
&m_s\ddot{y}_5 = -F_{y4} + F_{y6} - m_s g,\\
&I_s\ddot{\theta}_5 = -F_{x4}l_s\sin\theta_5 - F_{y4}l_s\cos\theta_5 - F_{x6}l_s\sin\theta_5 - F_{y6}l_s\cos\theta_5\\
&\qquad - T_{p4} - T_{p6} - T_{a4} - T_{a6},\\
&m_s\ddot{x}_6 = -F_{x5} + F_{x7},\\
&m_s\ddot{y}_6 = -F_{y5} + F_{y7} - m_s g,\\
&I_s\ddot{\theta}_6 = -F_{x5}l_s\sin\theta_6 - F_{y5}l_s\cos\theta_6 - F_{x7}l_s\sin\theta_6 - F_{y7}l_s\cos\theta_6\\
&\qquad - T_{p5} - T_{p7} - T_{a5} - T_{a7},\\
&m_f\ddot{x}_7 = -F_{x6} + F_{gx1} + F_{gx3},\\
&m_f\ddot{y}_7 = -F_{y6} + F_{gy1} + F_{gy3} - m_f g,\\
&I_f\ddot{\theta}_7 = -F_{x6}l_{f1}\sin\theta_7 - F_{y6}l_{f1}\cos\theta_7\\
&\qquad - F_{gx1}l_{f2}\sin(\alpha_1 - \theta_7) + F_{gy1}l_{f2}\cos(\alpha_1 - \theta_7)\\
&\qquad + F_{gx3}l_{f3}\sin(\theta_7 + \alpha_2) + F_{gy3}l_{f3}\cos(\theta_7 + \alpha_2)\\
&\qquad + T_{p6} + T_{a6},\\
&m_f\ddot{x}_8 = -F_{x7} + F_{gx2} + F_{gx4},\\
&m_f\ddot{y}_8 = -F_{y7} + F_{gy2} + F_{gy4} - m_f g,\\
&I_f\ddot{\theta}_8 = -F_{x7}l_{f1}\sin\theta_8 - F_{y7}l_{f1}\cos\theta_8\\
&\qquad - F_{gx2}l_{f2}\sin(\alpha_1 - \theta_8) + F_{gy2}l_{f2}\cos(\alpha_1 - \theta_8)\\
&\qquad + F_{gx4}l_{f3}\sin(\theta_8 + \alpha_2) + F_{gy4}l_{f3}\cos(\theta_8 + \alpha_2)\\
&\qquad + T_{p7} + T_{a7},
\end{aligned}
\tag{10}
$$

These equations can be written in compact form as (1) shown in the text.

The ground reaction forces are represented as a spring and damper acting at the heels and toes. The ground reaction forces in the horizontal and vertical directions are given as

$$F_{gxi} = \{-k_g(x_{fi} - x_{fti}) - b_g\dot{x}_{fi}\}\,1(y_g(x_{fti}) - y_{fi}),$$

$$F_{gyi} = \{-k_g(y_{fi} - y_g(x_{fti})) + b_g f(-\dot{y}_{fi})\}\,1(y_g(x_{fti}) - y_{fi}),$$

$$(i = 1,4)\quad 1(x) = \begin{cases} 1 & (0.01 < x) \\ 100x & (0 \leqslant x \leqslant 0.01), \\ 0 & (x < 0) \end{cases} \quad f(x) = \max(0, x), \tag{11}$$

where (x_{fi}, y_{fi}) indicate coordinates of the heels and toes which are represented by the positions and angles of the foot segments; $(x_{fti}, y_g(x_{fti}))$ indicate the rest position of the elastic forces, which are reset each time the heels and/or the toes touch the ground; $y_g(x)$ is a function of the ground profile that is established along the sagittal plane such that the elevation of the terrain changes horizontally; and k_g and b_g are coefficients of the spring and damper.

The torques exerted by passive joint structures are expressed by small viscous torques at each joint and large visco-elastic torques that limit the range of joint flexion and extension as

$$\begin{aligned}
T_{p1} &= b_1(\dot{\theta}_1 - \dot{\theta}_2) \\
&\quad + b_3 f(\theta_1 - \theta_2 - 7\pi/18)(\dot{\theta}_1 - \dot{\theta}_2) + k_1 f(\theta_1 - \theta_2 - 7\pi/18) \\
&\quad + b_3 f(\theta_2 - \theta_1 - \pi/9)(\dot{\theta}_1 - \dot{\theta}_2) - k_1 f(\theta_2 - \theta_1 - \pi/9), \\
T_{p2} &= b_2(\dot{\theta}_2 - \dot{\theta}_3) \\
&\quad + b_3 f(\theta_2 - \theta_3 - \pi/2)(\dot{\theta}_2 - \dot{\theta}_3) + k_2 f(\theta_2 - \theta_3 - \pi/2) \\
&\quad + b_3 f(\theta_3 - \theta_2 - \pi/9)(\dot{\theta}_2 - \dot{\theta}_3) - k_2 f(\theta_3 - \theta_2 - \pi/9), \\
T_{p3} &= b_2(\dot{\theta}_2 - \dot{\theta}_4) \\
&\quad + b_3 f(\theta_2 - \theta_4 - \pi/2)(\dot{\theta}_2 - \dot{\theta}_4) + k_2 f(\theta_2 - \theta_4 - \pi/2) \\
&\quad + b_3 f(\theta_4 - \theta_2 - \pi/9)(\dot{\theta}_2 - \dot{\theta}_4) - k_2 f(\theta_4 - \theta_2 - \pi/9), \\
T_{p4} &= -b_2(\dot{\theta}_3 - \dot{\theta}_5) \\
&\quad - b_4 f(\theta_3 - \theta_5)(\dot{\theta}_3 - \dot{\theta}_5) - k_1 f(\theta_3 - \theta_5) \\
&\quad - b_3 f(\theta_5 - \theta_3 - 5\pi/6)(\dot{\theta}_3 - \dot{\theta}_5) - k_1 f(\theta_5 - \theta_3 - 5\pi/6), \\
T_{p5} &= -b_2(\dot{\theta}_4 - \dot{\theta}_6) \\
&\quad - b_4 f(\theta_4 - \theta_6)(\dot{\theta}_4 - \dot{\theta}_6) - k_1 f(\theta_4 - \theta_6) \\
&\quad - b_3 f(\theta_6 - \theta_4 - 5\pi/6)(\dot{\theta}_4 - \dot{\theta}_6) + k_1 f(\theta_6 - \theta_4 - 5\pi/6), \\
T_{p6} &= b_2(\dot{\theta}_5 - \dot{\theta}_7) \\
&\quad + b_3 f(\theta_5 - \theta_7 - 0.5760 - 2\pi/9)(\dot{\theta}_5 - \dot{\theta}_7) \\
&\quad + k_1 f(\theta_5 - \theta_7 - 0.5760 - 2\pi/9) \\
&\quad + b_3 f(0.5760 - \theta_5 + \theta_7 - 5\pi/18)(\dot{\theta}_5 - \dot{\theta}_7) \\
&\quad - k_1 f(0.5760 - \theta_5 + \theta_7 - 5\pi/18), \\
T_{p7} &= b_2(\dot{\theta}_6 - \dot{\theta}_8) \\
&\quad + b_3 f(\theta_6 - \theta_8 - 0.5760 - 2\pi/9)(\dot{\theta}_6 - \dot{\theta}_8) \\
&\quad + k_1 f(\theta_6 - \theta_8 - 0.5760 - 2\pi/9) \\
&\quad + b_3 f(0.5760 - \theta_6 + \theta_8 - 5\pi/18)(\dot{\theta}_6 - \dot{\theta}_8) \\
&\quad - k_1 f(0.5760 - \theta_6 - \theta_8 - 5\pi/18),
\end{aligned} \tag{12}$$

where k_1 and k_2 are coefficients of the elastic torques and b_1, b_2, b_3, and b_4 are coefficients of the viscous torques.

B The equations of the kinematic constraints

The equations of the kinematic constraints are described by

$$\begin{aligned}
&x_1 + l_{H2}\cos\theta_1 = x_2 - l_p\cos\theta_2,\ y_1 - l_{H2}\sin\theta_1 = y_2 + l_p\sin\theta_2, \\
&x_2 + l_p\cos\theta_2 = x_3 - l_t\cos\theta_3,\ y_2 - l_p\sin\theta_2 = y_3 + l_t\sin\theta_3, \\
&x_2 + l_p\cos\theta_2 = x_4 - l_t\cos\theta_4,\ y_2 - l_p\sin\theta_2 = y_4 + l_t\sin\theta_4, \\
&x_3 + l_t\cos\theta_3 = x_5 - l_s\cos\theta_5,\ y_3 - l_t\sin\theta_3 = y_5 + l_s\sin\theta_5, \\
&x_4 + l_t\cos\theta_4 = x_6 - l_s\cos\theta_6,\ y_4 - l_t\sin\theta_4 = y_6 + l_s\sin\theta_6, \\
&x_5 + l_s\cos\theta_5 = x_7 - l_{f1}\cos\theta_7,\ y_5 - l_s\sin\theta_5 = y_7 + l_{f1}\sin\theta_7, \\
&x_6 + l_s\cos\theta_6 = x_8 - l_{f1}\cos\theta_8,\ y_6 - l_s\sin\theta_6 = y_8 + l_{f1}\sin\theta_8.
\end{aligned} \tag{13}$$

These equations can be written in compact form as (2) shown in the text. In order to reduce constraint forces in (1), (13) is differentiated twice, and we obtain:

$$\begin{aligned}
&\ddot{x}_1 - \ddot{x}_2 - l_{H2}\sin\theta_1\ddot{\theta}_1 - l_p\sin\theta_2\ddot{\theta}_2 = l_{H2}\cos\theta_1\dot{\theta}_1^2 + l_p\cos\theta_2\dot{\theta}_2^2, \\
&\ddot{y}_1 - \ddot{y}_2 - l_{H2}\cos\theta_1\ddot{\theta}_1 - l_p\cos\theta_2\ddot{\theta}_2 = -l_{H2}\sin\theta_1\dot{\theta}_1^2 - l_p\sin\theta_2\dot{\theta}_2^2, \\
&\ddot{x}_2 - \ddot{x}_3 - l_p\sin\theta_2\ddot{\theta}_2 - l_t\sin\theta_3\ddot{\theta}_3 = l_p\cos\theta_2\dot{\theta}_2^2 + l_t\cos\theta_3\dot{\theta}_3^2, \\
&\ddot{y}_2 - \ddot{y}_3 - l_p\cos\theta_2\ddot{\theta}_2 - l_t\cos\theta_3\ddot{\theta}_3 = -l_p\sin\theta_2\dot{\theta}_2^2 - l_t\sin\theta_3\dot{\theta}_3^2, \\
&\ddot{x}_2 - \ddot{x}_4 - l_p\sin\theta_2\ddot{\theta}_2 - l_t\sin\theta_4\ddot{\theta}_4 = l_p\cos\theta_2\dot{\theta}_2^2 + l_t\cos\theta_4\dot{\theta}_4^2, \\
&\ddot{y}_2 - \ddot{y}_4 - l_p\cos\theta_2\ddot{\theta}_2 - l_t\cos\theta_4\ddot{\theta}_4 = -l_p\sin\theta_2\dot{\theta}_2^2 - l_t\sin\theta_4\dot{\theta}_4^2, \\
&\ddot{x}_3 - \ddot{x}_5 - l_t\sin\theta_3\ddot{\theta}_3 - l_s\sin\theta_5\ddot{\theta}_5 = l_t\cos\theta_3\dot{\theta}_3^2 + l_s\cos\theta_5\dot{\theta}_5^2, \\
&\ddot{y}_3 - \ddot{y}_5 - l_t\cos\theta_3\ddot{\theta}_3 - l_s\cos\theta_5\ddot{\theta}_5 = -l_t\sin\theta_3\dot{\theta}_3^2 - l_s\sin\theta_5\dot{\theta}_5^2, \\
&\ddot{x}_4 - \ddot{x}_6 - l_t\sin\theta_4\ddot{\theta}_4 - l_s\sin\theta_6\ddot{\theta}_6 = l_t\cos\theta_4\dot{\theta}_4^2 + l_s\cos\theta_6\dot{\theta}_6^2, \\
&\ddot{y}_4 - \ddot{y}_6 - l_t\cos\theta_4\ddot{\theta}_4 - l_s\cos\theta_6\ddot{\theta}_6 = -l_t\sin\theta_4\dot{\theta}_4^2 - l_s\sin\theta_6\dot{\theta}_6^2, \\
&\ddot{x}_5 - \ddot{x}_7 - l_s\sin\theta_5\ddot{\theta}_5 - l_{f1}\sin\theta_7\ddot{\theta}_7 = l_s\cos\theta_5\dot{\theta}_5^2 + l_{f1}\cos\theta_7\dot{\theta}_7^2, \\
&\ddot{y}_5 - \ddot{y}_7 - l_s\cos\theta_5\ddot{\theta}_5 - l_{f1}\cos\theta_7\ddot{\theta}_7 = -l_s\sin\theta_5\dot{\theta}_5^2 - l_{f1}\sin\theta_7\dot{\theta}_7^2, \\
&\ddot{x}_6 - \ddot{x}_8 - l_s\sin\theta_6\ddot{\theta}_6 - l_{f1}\sin\theta_8\ddot{\theta}_8 = l_s\cos\theta_6\dot{\theta}_6^2 + l_{f1}\cos\theta_8\dot{\theta}_8^2, \\
&\ddot{y}_6 - \ddot{y}_8 - l_s\cos\theta_6\ddot{\theta}_6 - l_{f1}\cos\theta_8\ddot{\theta}_8 = -l_s\sin\theta_6\dot{\theta}_6^2 - l_{f1}\sin\theta_8\dot{\theta}_8^2.
\end{aligned} \tag{14}$$

C The torques exerted by the muscles

The active torques at each joint are given as a function of the torques exerted by the 20 muscles:

$$\begin{aligned}
T_{a1} &= T_{m2} - T_{m1}, \\
T_{a2} &= T_{m4} - T_{m3} + T_{m8} - T_{m7}, \\
T_{a3} &= T_{m6} - T_{m5} + T_{m10} - T_{m9}, \\
T_{a4} &= T_{m12} - T_{m11} + \varepsilon_1 T_{m7} - \varepsilon_2 T_{m8} - \varepsilon_3 T_{m19}, \\
T_{a5} &= T_{m14} - T_{m13} + \varepsilon_1 T_{m9} - \varepsilon_2 T_{m10} - \varepsilon_3 T_{m20}, \\
T_{a5} &= T_{m16} - T_{m15} + T_{m19}, \\
T_{a7} &= T_{m18} - T_{m17} + T_{m20}
\end{aligned} \tag{15}$$

where ε_1, ε_2, and ε_3 shows the proportions of one torque to the other of the two-joint muscles. These can be written in compact form as (3) in the text.

D Numerical methods

Equation (1) can be transformed into a compact form as

$$\ddot{\varphi} = \Omega(\varphi)\mathbf{F} + \Psi(\varphi, \dot{\varphi}, \mathbf{F}_g(\varphi, \dot{\varphi}, \mathbf{x}_{ft}), \mathbf{T}_p(\varphi, \dot{\varphi}), \mathbf{T}_a) \tag{16}$$

where φ is a (24×1) vector of the inertial positions and angles of 8 segments; Ω is a (24×14) matrix; ψ is a (14×1) vector.

Equation (14) can be written in compact form as

$$\Phi(\varphi)\ddot{\varphi} = \eta(\varphi, \dot{\varphi}) \tag{17}$$

where Φ is a (14×24) matrix and η is a (14×1) vector.

By eliminating $\mathbf{F}$ from (16) and (17), we obtain

$$\ddot{\varphi} = \Omega(\varphi)[\Phi(\varphi)\Omega(\varphi)]^{-1} \times [\eta(\varphi,\dot{\varphi}) - \Phi(\varphi)\Psi(\varphi,\dot{\varphi},\mathbf{F}_g(\varphi,\dot{\varphi},\mathbf{x}_{ft}),\mathbf{T}_p(\varphi,\dot{\varphi}),\mathbf{T}_a)] + \Psi(\varphi,\dot{\varphi},\mathbf{F}_g(\varphi,\dot{\varphi},\mathbf{x}_{ft}),\mathbf{T}_p(\varphi,\dot{\varphi}),\mathbf{T}_a)] \tag{18}$$

This equation can be numerically integrated, given the active torques $\mathbf{T}_a$.

The method called speed stabilization through projection (Ekeberg 1993) was incorporated to avoid numerical errors caused by a violation of the kinematical constraints. By projecting the speed values down to the subspace formed by the kinematic constraints, the speed values are adjusted as

$$\tilde{\dot{\varphi}} = \dot{\varphi} - \Omega(\varphi)[\Phi(\varphi)\Omega(\varphi)]^{-1}\Phi(\varphi)\dot{\varphi} \tag{19}$$

where $\tilde{\dot{\varphi}}$ is the value of speed that is replaced with the former ones at every time step of the numerical integration.

E The global angle

The coordinate of the body's center of gravity (COG) is given by

$$x_{cg} = \sum_{i=1}^{8} m_i x_i \Big/ \sum_{i=1}^{8} m_i, \quad y_{cg} = \sum_{i=1}^{8} m_i y_i \Big/ \sum_{i=1}^{8} m_i \tag{20}$$

By differentiation of the above equations with respect to time, we obtain

$$\dot{x}_{cg} = \sum_{i=1}^{8} m_i \dot{x}_i \Big/ \sum_{i=1}^{8} m_i, \quad \dot{y}_{cg} = \sum_{i=1}^{8} m_i \dot{y}_i \Big/ \sum_{i=1}^{8} m_i \tag{21}$$

The coordinate of the center of pressure (COP) is represented as

$$x_{cp} = \sum_{i=1}^{4} F_{gyi} x_{ri} \Big/ \sum_{i=1}^{4} F_{gyi}, \quad y_{cp} = y_g(x_{cp}) \tag{22}$$

The global angle was defined as Eq. (5) in the text.

The global angular velocity is defined as

$$\dot{\phi} = \{(y_{cg} - y_{cp})\dot{x}_{cg} + (x_{cp} - x_{cg})\dot{y}_{cg}\} / \{(x_{cp} - x_{cg})^2 + (y_{cp} - y_{cg})^2\} \tag{23}$$

F The global states

The alteration of the foot contacting the ground can be expressed by

$$\begin{aligned} &s_{ron} = 1(F_{gy1} + F_{gy3}), \quad s_{roff} = 1 - s_{ron}, \\ &s_{lon} = 1(F_{gy2} + F_{gy4}), \quad s_{loff} = 1 - s_{lon} \\ &s_r = 1(x_{f1} - x_{f2}), \quad s_l = 1(x_{f2} - x_{f1}) \end{aligned} \tag{24}$$

The 'global states' which were defined in the text can be written by

$$\begin{aligned} &s_{g1} = s_{ron}s_{lon}s_r, \quad s_{g2} = s_{ron}s_{loff}1(\pi/2 - \phi), \quad s_{g3} = s_{ron}s_{loff}1(\phi - \pi/2), \\ &s_{g4} = s_{lon}s_{ron}s_l, \quad s_{g5} = s_{lon}s_{roff}1(\pi/2 - \phi), \quad s_{g6} = s_{lon}s_{roff}1(\phi - \pi/2) \end{aligned} \tag{25}$$

The first and second half of a gait cycle are described by

$$s_{rst} = s_{g1} + s_{g2} + s_{g3}, \quad s_{lst} = s_{g4} + s_{g5} + s_{g6} \tag{26}$$

G State-dependent couplings among the neural oscillators

The input signal from other neurons to each neuron is given as

$$\begin{aligned} Q_1 &= s_{g2}w_1 f(u_4) + s_{g5}w_1 f(u_6), \\ Q_2 &= s_{g3}w_1 f(u_3) + s_{g6}w_1 f(u_5), \\ Q_3 &= (s_{g4} + s_{g5} - s_{g6})w_1 f(u_7) + (-s_{g1} - s_{g2} + s_{g3})w_1 f(u_8) \\ &\quad + (-s_{g1} - s_{g2} + s_{g5})w_1 f(u_{11}) + (s_{g3} + s_{g4} - s_{g6})w_1 f(u_{12}), \\ Q_4 &= -Q_3, \\ Q_5 &= (s_{g1} + s_{g2} - s_{g3})w_1 f(u_9) + (-s_{g4} - s_{g5} + s_{g6})w_1 f(u_{10}) \\ &\quad + (-s_{g4} - s_{g5} + s_{g2})w_1 f(u_{13}) + (s_{g6} + s_{g1} - s_{g3})w_1 f(u_{14}), \\ Q_6 &= -Q_5, \\ Q_7 &= (-s_{g3} + s_{g4} + s_{g5})w_2 f(u_3) + (-s_{g1} - s_{g2} + s_{g6})w_2 f(u_4) \\ &\quad + (-s_{g1} - s_{g2} + s_{g5})w_1 f(u_{11}) + (-s_{g3} + s_{g4} + s_{g6})w_1 f(u_{12}), \\ Q_8 &= -Q_7, \\ Q_9 &= (-s_{g6} + s_{g1} + s_{g2})w_2 f(u_5) + (-s_{g4} - s_{g5} + s_{g3})w_2 f(u_6) \\ &\quad + (-s_{g4} - s_{g5} + s_{g2})w_1 f(u_{13}) + (-s_{g6} + s_{g1} + s_{g3})w_1 f(u_{14}), \\ Q_{10} &= -Q_9, \\ Q_{11} &= (-s_{g3} - s_{g4} + s_{g5})w_2 f(u_3) + (s_{g1} + s_{g2} - s_{g6})w_2 f(u_4) \\ &\quad + (-s_{g4} + s_{g5} - s_{g6})w_1 f(u_7) + (s_{g1} + s_{g2} - s_{g3})w_1 f(u_8), \\ Q_{12} &= -Q_{11}, \\ Q_{13} &= (-s_{g6} - s_{g1} + s_{g2})w_2 f(u_5) + (s_{g4} + s_{g5} - s_{g3})w_2 f(u_6) \\ &\quad + (-s_{g1} + s_{g2} - s_{g3})w_1 f(u_9) + (s_{g4} + s_{g5} - s_{g6})w_1 f(u_{10}), \\ Q_{14} &= -Q_{13} \end{aligned} \tag{27}$$

where w_1 and w_2 show the coupling strength. These equations can be written in compact form as (6) in the text.

H State-dependent inputs of sensory signals

The input signal to each neuron is represented by

$$\begin{aligned} S_1 &= -q_1(\theta_1 - 0.55\pi) - q_2\dot{\theta}_1, \\ S_2 &= -S_1, \\ S_3 &= q_3(\theta_3 - \pi/2) + s_{lst}q_4(\theta_5 - \pi/2) + (s_{rst} - s_{lst})q_5(\phi - \pi/2), \\ S_4 &= -S_3, \\ S_5 &= q_3(\theta_4 - \pi/2) + s_{rst}q_4(\theta_6 - \pi/2) + (s_{lst} - s_{rst})q_5(\phi - \pi/2), \\ S_6 &= -S_5, \\ S_7 &= q_4(\theta_5 - \pi/2) + (-s_{rst} + s_{lst})q_5 f(\pi/2 - \phi), \\ S_8 &= -S_7, \\ S_9 &= q_4(\theta_6 - \pi/2) + (-s_{lst} + s_{rst})q_5 f(\pi/2 - \phi), \\ S_{10} &= -S_9, \\ S_{11} &= s_{roff}q_6(\theta_7 - 0.9948) - s_{rst}q_4(\theta_5 - \pi/2) \\ &\quad - (s_{rst} + s_{g5} + s_{g6})q_5(\phi - \pi/2) - s_{g4}q_5 f(\pi/2 - \phi) \\ &\quad - (s_{g1}q_7 + s_{g3}q_8)\dot{\phi}, \\ S_{12} &= -S_{11}, \\ S_{13} &= s_{loff}q_6(\theta_8 - 0.9948) - s_{lst}q_4(\theta_6 - \pi/2) \\ &\quad - (s_{lst} + s_{g2} + s_{g3})q_5(\phi - \pi/2) - s_{g1}q_5 f(\pi/2 - \phi) \\ &\quad - (s_{g4}q_7 + s_{g6}q_8)\dot{\phi}, \\ S_{14} &= -S_{13} \end{aligned} \tag{28}$$

where q_i ($i = 1, 8$) shows strength of inputs. These equations are written in compact form as (7).

I Generation of the motor commands

The muscle torques generated by the output of the neural rhythm generator are given as

$$T_{mr1} = p_1 f(u_1), \quad T_{mr2} = p_2 f(u_2),$$

$$T_{mr3} = (s_{ron} p_3 + s_{roff} p_4) f(u_3), \quad T_{mr4} = (s_{ron} p_5 + s_{roff} p_6) f(u_4),$$

$$T_{mr5} = (s_{lon} p_3 + s_{loff} p_4) f(u_5), \quad T_{mr6} = (s_{lon} p_5 + s_{loff} p_6) f(u_6),$$

$$T_{mr7} = (s_{ron} p_7 + s_{roff} p_8) f(u_3), \quad T_{mr8} = (s_{ron} p_9 + s_{roff} p_{10}) f(u_4),$$

$$T_{mr9} = (s_{lon} p_7 + s_{loff} p_8) f(u_5), \quad T_{mr10} = (s_{lon} p_9 + s_{loff} p_{10}) f(u_6), \quad (29)$$

$$T_{mr11} = s_{lst} p_{11} f(u_7), \quad T_{mr12} = (s_{ron} p_{12} + s_{roff} p_{13}) f(u_8),$$

$$T_{mr13} = s_{rst} p_{11} f(u_9), \quad T_{mr14} = (s_{lon} p_{12} + s_{loff} p_{13}) f(u_{10}),$$

$$T_{mr15} = (s_{ron} p_{14} + s_{roff} p_{15}) f(u_{11}), \quad T_{mr16} = (s_{ron} p_{16} + s_{roff} p_{17}) f(u_{12}),$$

$$T_{mr17} = (s_{lon} p_{14} + s_{loff} p_{15}) f(u_{13}), \quad T_{mr18} = (s_{lon} p_{16} + s_{loff} p_{17}) f(u_{14}),$$

$$T_{mr19} = s_{ron} p_{18} f(u_{12}), \quad T_{mr20} = s_{lon} p_{18} f(u_{14})$$

where $p_i (i = 1, 18)$ shows constant parameters which determine the strength of torques.

The muscle torques generated by the impedance controller are given by

$$T_{mi1} = p_{i1} f(\theta_2 - \theta_1) + p_{i2} f(\dot{\theta}_2 - \dot{\theta}_1),$$

$$T_{mi2} = p_{i1} f(\theta_1 - \theta_2) + p_{i2} f(\dot{\theta}_1 - \dot{\theta}_2),$$

$$T_{mi3} = s_{ron} p_{i3} f(0.55\pi - \theta_2) + s_{ron} p_{i4} f(-\dot{\theta}_2),$$

$$T_{mi4} = s_{ron} p_{i3} f(\theta_2 - 0.55\pi) + s_{ron} p_{i4} f(\dot{\theta}_2),$$

$$T_{mi5} = s_{lon} p_{i3} f(0.55\pi - \theta_2) + s_{lon} p_{i4} f(-\dot{\theta}_2),$$

$$T_{mi6} = s_{lon} p_{i3} f(\theta_2 - 0.55\pi) + s_{lon} p_{i4} f(\dot{\theta}_2), \quad (30)$$

$$T_{mi7} = 0.0, \quad T_{mi8} = 0.0, \quad T_{mi9} = 0.0, \quad T_{mi10} = 0.0,$$

$$T_{mi11} = 0.0, \quad T_{mi12} = s_{rst} p_{i5} f(\theta_5 - \theta_3) + s_{rst} p_{i6} f(\dot{\theta}_5 - \dot{\theta}_3),$$

$$T_{mi13} = 0.0, \quad T_{mi14} = s_{lst} p_{i5} f(\theta_6 - \theta_4) + s_{lst} p_{i6} f(\dot{\theta}_6 - \dot{\theta}_4),$$

$$T_{mi15} = s_{rst} p_{i7} f(\dot{\theta}_7 - \dot{\theta}_5), \quad T_{mi16} = s_{rst} p_{i7} f(\dot{\theta}_5 - \dot{\theta}_7),$$

$$T_{mi17} = s_{lst} p_{i7} f(\dot{\theta}_8 - \dot{\theta}_6), \quad T_{mi18} = s_{lst} p_{i7} f(\dot{\theta}_6 - \dot{\theta}_8),$$

$$T_{mi19} = 0.0, \quad T_{mi20} = 0.0$$

where $p_{ii} (i = 1, 7)$ shows constant parameters which determine the strength of torques.

J Simulation parameters

(aα) The body parameters and the ground parameters

$m_H = 38.0$, $l_{H1} = 0.4$, $l_{H2} = 0.3$,

$I_H = 1.1399$, $m_p = 10.0$, $l_p = 0.1$, $I_p = 0.05$,

$m_t = 7.0$, $l_t = 0.2$, $l_t = 0.0933$, $m_s = 3.0$,

$l_s = 0.2$, $I_s = 0.0399$,

$m_f = 1.0$, $l_{f1} = 0.08$, $l_{f2} = 0.12$, $l_{f3} = 0.10$,

$\alpha_1 = 1.22$, $\alpha_2 = 2.44$, $I_f = 0.0032$,

$k_1 = 1000.0$, $k_2 = 500.0$, $b_1 = 10.0$, $b_2 = 1.0$, $b_3 = 100.0$, $b_4 = 1000.0$,

$\varepsilon_1 = 1.0$, $\varepsilon_2 = 0.5$, $\varepsilon_3 = 1.0$, $g = 9.8$, $k_g = 30000.0$, $b_g = 1000.0$

(b) The parameters in the neural oscillators

$\tau_1 = \tau_2 = 1/32$, $\tau_i = 1/18$ $(i = 3, 14)$,

$\tau'_1 = \tau'_2 = 1/2.656$, $\tau_i = 1/1.494$ $(i = 3, 14)$,

$w^0_{2i-1\,2i} = w^0_{2i\,2i-1} = -2.0$ $(i = 1, 7)$,

$\beta = 2.5$, $u_0 = 6.0$

(c) The strength of the neural connections

$w^0_{3\,5} = w^0_{5\,3} = w^0_{4\,6} = w^0_{6\,4} = w^0_{7\,9} = w^0_{9\,7} = w^0_{8\,10} = w^0_{10\,8} = -1.0$;

$w^0_{11\,13} = w^0_{13\,11} = w^0_{12\,14} = w^0_{14\,12} = -0.2$,

$w^0_{2\,4} = w^0_{2\,6} = 1.0$; $w_1 = 0.1$, $w_2 = 0.2$

(d) The magnitude of the coefficients in the rhythmic force controller

$p_1 = 5.0$, $p_2 = 10.0$, $p_3 = 4.0$, $p_4 = 2.0$, $p_5 = 15.0$

$p_6 = 4.0$, $p_7 = 3.0$, $p_8 = 2.0$, $p_9 = 15.0$,

$p_{10} = 8.0$, $p_{11} = 2.0$, $p_{12} = 3.0$, $p_{13} = 2.0$, $p_{14} = 8.0$,

$p_{15} = 1.5$, $p_{16} = 12.0$, $p_{17} = 1.0$, $p_{18} = 7.0$

(e) The strength of the sensory inputs

$q_1 = 6.0$, $q_2 = 0.9$, $q_3 = 1.5$, $q_4 = 1.5$, $q_5 = 3.0$,

$q_6 = 3.0$, $q_7 = 0.1$, $q_8 = 0.2$

(f) The impedance parameters

$p_{i1} = 500.0$, $p_{i2} = 10.0$, $p_{i3} = 800.0$, $p_{i4} = 20.0$,

$p_{i5} = 150.0$, $p_{i6} = 10.0$, $p_{i7} = 10.0$

K Initial conditions

(a) The musculoskeletal system

$x_2 = 1.000$, $y_2 = 0.984$, $\dot{x}_2 = 0.7$, $\dot{y}_2 = 0.0$,

$\theta_1 = 1.714$, $\theta_2 = 1.588$, $\theta_3 = 0.653$, $\theta_4 = 1.618$,

$\theta_5 = 1.418$, $\theta_6 = 1.623$, $\theta_7 = 0.543$, $\theta_8 = 0.984$,

$\dot{\theta}_1 = 0.0$, $\dot{\theta}_2 = 0.0$, $\dot{\theta}_3 = -1.0$, $\dot{\theta}_4 = 1.0$, $\dot{\theta}_5 = -5.0$,

$\dot{\theta}_6 = 2.0$, $\dot{\theta}_7 = -8.0$, $\dot{\theta}_8 = 0.0$

The positions and velocities of the other segments can be calculated by using the equations of kinematic constraints.

(b) The neural rhythm generator

$u_1 = 1.0$, $u_2 = -1.0$, $u_3 = -1.0$, $u_4 = 1.0$,

$u_5 = 1.0$, $u_6 = 1.0$, $u_7 = 1.0$, $u_8 = -1.0$,

$u_9 = -1.0$, $u_{10} = 1.0$, $u_{11} = 1.0$,

$u_{12} = -1.0$, $u_{13} = 1.0$, $u_{14} = -1.0$,

$v_i = 1.0$ $(i = 1, 14)$

References

Andersson O, Grillner S (1983) Peripheral control of the cat's step cycle. II. Entrainment of the central pattern generators for locomotion by sinusoidal hip movements during 'fictive locomotion'. Acta Physiol Scand 118:229–239

Arshavsky YI, Gelfand IM, Orlovsky GN (1984) Cerebellum and rhythmical movements. Springer, Berlin Heidelberg New York

Bässler U (1986) On the definition of central pattern generator and its sensory control. Biol Cybern 54:65–69

Beer RD (1990) Intelligence as adaptive behavior. Academic Press, New York

Berger W, Dietz V, Quintern J (1984) Corrective reactions to stumbling in man: neuronal co-ordination of bilateral leg muscle activity during gait. J Physiol 357:109–125

Clark JE, Phillips SJ (1993) A longitudinal study of intralimb coordination in the first year of independent walking: a dynamical systems analysis. Child Dev 64:1143–1157
Crowninshield RD, Brand RA (1981) A physiologically based criterion of muscle force prediction in locomotion. J Biomech 14-11:793–801
Cruse H (1990) What mechanisms coordinate leg movement in walking arthropods? Trends Neurosci 13:15–21
Davis BL, Vaughan CL (1993) Phasic behavior of EMG signals during gait: use of multivariate statistics. J Electromyogr Kinesiol 3:51–60
Davy DT, Audu ML (1987) A dynamic optimization technique for predicting muscle forces in the swing phase of gait. J Biomech 20:187–201
Delcomyn F (1980) Neural basis of rhythmic behavior in animals. Science 210:492–498
Dietz V (1992) Human neuronal control of automatic functional movements: interaction between central programs and afferent input. Physiol Rev 72:33–69
Doya K, Yoshizawa S (1992) Adaptive synchronization of neural and physical oscillators. In: Moody JE, Hanson SJ, Lippmann RP (eds) Advances in neural information processing systems 4. Morgan Kaufmann, San Mateo, 109–116
Ekeberg Ö (1993) A combined neuronal and mechanical model of fish swimming. Biol Cybern 69:363–374
Flashner H, Beuter A, Arabyan A (1987) Modeling of control and learning in a stepping motion. Biol Cybern 55:387–396
Forssberg H (1979) Stumbling corrective reaction: a phase-dependent compensatory reaction during locomotion. J Neurophysiol 42:936–953
Forssberg H (1985) Ontogeny of human locomotor control. I. Infant stepping, supported locomotion and transition to independent locomotion. Exp Brain Res 57:480–493
Grillner S (1985) Neurobiological bases of rhythmic motor acts in vertebrates. Science 228:143–149
Grillner S, Matsushima T (1991) The neural network underlying locomotion in lamprey – synaptic and cellular mechanisms. Neuron 7:1–15
Grillner S, Wallen P (1982) On peripheral control mechanisms acting on the central pattern generators for swimming in the dogfish. J Exp Biol 98:1–22
Haken H, Kelso JAS, Bunz H (1985) A theoretical model of phase transitions in human hand movements. Biol Cybern 51:347–356
Hatze H (1976) The complete optimization of a human motion. Math Biosci 28:99–135
Hogan N (1985) The mechanics of multi-joint posture and movement control. Biol Cybern 52:315–331
Holt KG, Hamill J, Andres RO (1990) The force-driven harmonic oscillator as a model for human locomotion. Hum Mov Sci 9:55–68
Inman VT, Ralston HJ, Todd F (1981) Human walking. Williams & Wikins, Baltimore
Kawahara K, Mori S (1982) A two compartment model of the stepping generator: analysis of the roles of a stage-setter and a rhythm generator. Biol Cybern 43:225–230
Kimura S, Yano M, Shimizu H (1993) A self-organizing model of walking patterns of insects. Biol Cybern 69:183–193
Leonard CT, Hirschfeld H, Forssberg H (1991) The development of independent walking in children with cerebral palsy. Dev Med Child Neurol 33:567–577
Macpherson JM (1988) Strategies that simplify the control of quadrupedal stance. I. Forces at the ground. J Neurophysiol 60:204–217
Maioli C, Poppele RE (1991) Parallel processing of multisensory information concerning self-motion. Exp Brain Res 87:119–125
Matsuoka K (1985) Sustained oscillations generated by mutually inhibiting neurons with adaptation. Biol Cybern 52:367–376
Matthews PBC (1991) The human stretch reflex and the motor cortex. Trends Neurosci 14:87–91
McGeer (1993) Dynamics and control of bipedal locomotion. J Theor Biol 163:277–314
McGraw MB (1940) Neuromuscular development of the human infant as exemplified in achievement of erect locomotion. J Pediatr 17:747–771
McMahon TA (1984) Muscles, reflexes, and locomotion. Princeton Univ Press, Princeton
Miller S, Scott PD (1977) The spinal locomotor generator. Exp Brain Res 30:387–403
Mochon S, McMahon TA (1980) Ballistic walking. J Biomech 13: 49–57
Mori S (1987) Integration of posture and locomotion in acute decerebrate cats and in awake, freely moving cats. Prog Neurobiol 28:161–195
Murray MP (1967) Gait as a total pattern of movement. Am J Phys Med 46:290–333
Nashner LM, McCollum G (1985) The organization of human postural movements: a formal basis and experimental synthesis. Behav Brain Sci 8:135–172
Nilsson J, Thorstensson (1989) Ground reaction forces at different speeds of human walking and running. Acta Physiol Scand 136:217–227
Nilsson J, Thorstensson A, Halbertsma J (1985) Changes in leg movements and muscle activity with speed of locomotion and mode of progression in humans. Acta Physiol Scand 123:457–475
Onyshko S, Winter DA (1980) A mathematical model for the dynamics of human locomotion. J Biomech 13:361–368
Pandy M, Berme N (1988) A numerical method for simulating the dynamics of human walking. J Biomech 21:1043–1051
Patla AE (1988) Analytic approaches to the study of outputs from central pattern generators In: Cohen AH, Rossignol S, Grillner S (eds) Neural control of rhythmic movements in vertebrates. Wiley, New York, pp 455–486
Pearson KG, Ramirez JM, Jiang W (1992) Entrainment of locomotor rhythm by group Ib afferents from ankle extensor muscles in spinal cats. Exp Brain Res 90:557–566
Raibert MH (1984) Hopping in legged systems-modeling and simulation for the two-dimensional one-legged case. IEEE Trans SMC 14:451–463
Schöner G, Kelso JAS (1988) Dynamic pattern generation in behavioral and neural systems. Science 239:1513–1520
Selverston AI (ed) (1985) Model neural networks and behavior. Plenum, New York
Smith JL, Zernicke RF (1987) Predictions for neural control based on limb dynamics. Trends Neurosci 10:123–128
Soechting FF, Flanders M (1992) Moving in three-dimensional space: frames of references, vectors, and coordinate systems. Annu Rev Neurosci 15:167–191
Stein RB, Capaday C (1988) The modulation of human reflexes during functional motor tasks. Trends Neurosci 11:328–332
Taga G (1994) Emergence of bipedal locomotion through entrainment among the neuro-musculo-skeletal system and the environment. Physica D 75:190–208
Taga G, Yamaguchi Y, Shimizu H (1991) Self-organized control of bipedal locomotion by neural oscillators in unpredictable environment. Biol Cybern 65:147–159
Thelen E (1988) Dynamical approaches to the development of behavior. In: Kelso JAS, Mandell AJ, Shlesinger MF (eds) Dynamic patterns in complex systems. World Scientific, New York, pp 348–369
Thelen E, Fisher DM (1982) Newborn stepping: an explanation for a 'disappearing' reflex. Dev Psychol 18:760–775
Vukobratovic M, Stokic D (1975) Dynamic control of unstable locomotion robots. Math Biosci 24:129–157
Wendler G (1974) The influence of proprioceptive feedback on locust flight coordination. J Comp Physiol 88:173–200
Williams TL, Sigvardt KA, Kopell N, Ermentrout GB, Remler MP (1990) Forcing of coupled nonlinear oscillators: studies of intersegmental coordination in the lamprey locomotor central pattern generator. J Neurophysiol 64:862–871
Winstein CJ, Garfinkel A (1989) Qualitative dynamics of disordered human locomotion: a preliminary investigation. J Mot Behav 21:373–391
Winter DA (1987) Biomechanics and motor control of human gait. University of Waterloo Press
Yamaguchi GT, Zajac FE (1990) Restoring unassisted natural gait to paraplegics via functional neuromuscular stimulation: a computer simulation study. IEEE Trans BME 37:886–902
Yamazaki N (1991) Energy consumption in human musculoskeletal system during walking (in Japanese). Proc SICE Symp Decentralized Autonomous Systems, 19–22
Yoon YS, Mansour JM (1982) The passive elastic moment at the hip. J Biomech 15:905–910